The Ubiquitous Aldehyde Reductase (AKR1A1) Oxidizes Proximate Carcinogen *trans*-Dihydrodiols to *o*-Quinones: Potential Role in Polycyclic Aromatic Hydrocarbon Activation†

Nisha T. Palackal,‡ Michael E. Burczynski,‡,§ Ronald G. Harvey,|| and Trevor M. Penning*,‡

Departments of Biochemistry and Biophysics and Pharmacology, University of Pennsylvania School of Medicine, Philadelphia, Pennsylvania 19104, and The Ben May Institute for Cancer Research, University of Chicago, Chicago, Illinois 60637

Received April 30, 2001; Revised Manuscript Received July 6, 2001

ABSTRACT: Polycyclic aromatic hydrocarbons (PAHs) are metabolized to *trans*-dihydrodiol proximate carcinogens by human epoxide hydrolase (EH) and CYP1A1. Human dihydrodiol dehydrogenase isoforms (AKR1C1−AKR1C4), members of the aldo−keto reductase (AKR) superfamily, activate *trans*-dihydrodiols by converting them to reactive and redox-active *o*-quinones. We now show that the constitutively and widely expressed human AKR, aldehyde reductase (AKR1A1), will oxidize potent proximate carcinogen *trans*-dihydrodiols to their corresponding *o*-quinones. cDNA encoding AKR1A1 was isolated from HepG2 cells, overexpressed in *Escherichia coli*, purified to homogeneity, and characterized. AKR1A1 oxidized the potent proximate carcinogen (±)-*trans*-7,8-dihydroxy-7,8-dihydrobenzo[*a*]pyrene with a higher utilization ratio (V_{max}/K_m) than any other human AKR. AKR1A1 also displayed a high V_{max}/K_m for the oxidation of 5-methylchrysene-7,8-diol, benz[*a*]anthracene-3,4-diol, 7-methylbenz[*a*]anthracene-3,4-diol, and 7,12-dimethylbenz[*a*]anthracene-3,4-diol. AKR1A1 displayed rigid regioselectivity by preferentially oxidizing non-K-region *trans*-dihydrodiols. The enzyme was stereoselective and oxidized 50% of each racemic PAH *trans*-dihydrodiol tested. The absolute stereochemistries of the reactions were assigned by circular dichroism spectrometry. AKR1A1 preferentially oxidized the metabolically relevant (−)-benzo[*a*]pyrene-7(*R*),8(*R*)-dihydrodiol. AKR1A1 also preferred (−)-benz[*a*]anthracene-3(*R*),4(*R*)-dihydrodiol, (+)-7-methylbenz[*a*]anthracene-3(*S*),4(*S*)-dihydrodiol, and (−)-7,12-dimethylbenz[*a*]anthracene-3(*R*),4(*R*)-dihydrodiol. The product of the AKR1A1-catalyzed oxidation of (±)-*trans*-7,8-dihydroxy-7,8-dihydrobenzo[*a*]pyrene was trapped with 2-mercaptoethanol and characterized as a thioether conjugate of benzo[*a*]pyrene-7,8-dione by LC/MS. Multiple human tissue expression array analysis showed coexpression of AKR1A1, CYP1A1, and EH, indicating that *trans*-dihydrodiol substrates are formed in the same tissues in which AKR1A1 is expressed. The ability of this general metabolic enzyme to divert *trans*-dihydrodiols to *o*-quinones suggests that this pathway of PAH activation may be widespread in human tissues.

PAHs[1] are ubiquitous environmental pollutants and procarcinogens which require metabolic activation to electrophiles to exert their deleterious effects (*1*). Of the mixture of PAH present in tobacco smoke, benzo[*a*]pyrene is a major component (*3*). This representative PAH is metabolized by monoxygenases (CYP P450) to phenols and 1,6-, 3,6-, and 6,12-diones. However, these major metabolites do not account for the carcinogenicity of PAH (*3*). Instead, three principal routes of activation have been proposed.

The first route involves the formation of radical cations (*4*) at the most electrophilic carbon by CYP-peroxidase in the presence of a peroxide substrate. The remaining two pathways both require CYPs to form arene oxides on the terminal benzo ring. Subsequent hydrolysis by epoxide

† This research was supported by NIH Grant CA39504 to T.M.P. N.T.P. received a Bristol Myers Squibb Young Investigator Award for a preliminary account of this work at the 90th Annual Meeting of the American Association for Cancer Research, Philadelphia, PA, April 10−14, 1999.

* To whom correspondence and requests for reprints should be addressed at the Department of Pharmacology, University of Pennsylvania School of Medicine, 3620 Hamilton Walk, Philadelphia, PA 19104-6084. Tel: (215) 898-9445. Fax: (215) 573-2236. E-mail: penning@pharm.med.upenn.edu.

‡ University of Pennsylvania School of Medicine.

§ Current address: Wyeth Ayerst Research, Genetics Institute, One Burtt Rd, Andover MA 01810.

|| University of Chicago.

[1] Abbreviations: PAH, polycyclic aromatic hydrocarbon; CD, circular dichroism; LC/MS, liquid chromatography/mass spectrometry; aldehyde reductase, EC 1.1.1.2 (also designated AKR1A1); 3α-HSD/DD, 3α-hydroxysteroid dehydrogenase/dihydrodiol dehydrogenase; CYP1A1, cytochrome P450 1A1; EH, epoxide hydrolase; SQ, *o*-semiquinone anion; MTE, multiple tissue expression; BP-7,8-diol, (±)-*trans*-7,8-dihydroxy-7,8-dihydrobenzo[*a*]pyrene; *anti*-BPDE, (±)-*anti*-7,8-dihydroxy-9α,10α-epoxy-7,8,9,10-tetrahydrobenzo[*a*]pyrene; BPQ, BP-7,8-dione; NP-1,2-diol, (±)-*trans*-1,2-dihydroxy-1,2-dihydronaphthalene; Ph-1,2-diol, (±)-*trans*-1,2-dihydroxy-1,2-dihydrophenanthrene; Ph-9,10-diol, (±)-*trans*-9,10-dihydroxy-9,10-dihydrophenanthrene; C-1,2-diol, (±)-*trans*-1,2-dihydroxy-1,2-dihydrochrysene; 5-MC-7,8-diol, (±)-*trans*-7,8-dihydroxy-7,8-dihydro-5-methylchrysene; BA-3,4-diol, (±)-*trans*-3,4-dihydroxy-3,4-dihydrobenz[*a*]anthracene; 7-MBA-3,4-diol, (±)-*trans*-3,4-dihydroxy-3,4-dihydro-7-methylbenz[*a*]anthracene; 12-MBA-3,4-diol, (±)-*trans*-3,4-dihydroxy-3,4-dihydro-12-methylbenz[*a*]-anthracene; 7,12-DMBA-3,4-diol, (±)-*trans*-3,4-dihydroxy-3,4-dihydro-7,12-dimethylbenz[*a*]anthracene; B[*c*]P-3,4-diol, (±)-*trans*-3,4-dihydroxy-3,4-dihydrobenzo[*c*]phenanthrene; B[*g*]C-11,12-diol, (±)-*trans*-11,12-dihydroxy-11,12-dihydrobenzo[*g*]chrysene; ROS, reactive oxygen species.

10.1021/bi010872t CCC: $20.00
Published on Web 08/14/2001

Scheme 1: Metabolic Activation of PAH *trans*-Dihydrodiols

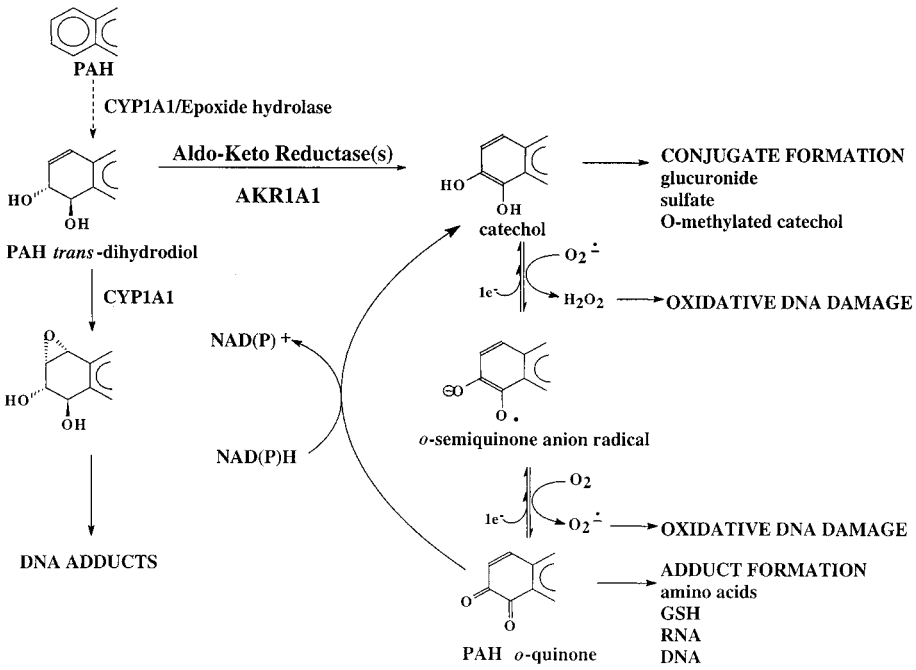

hydrolase (EH) results in the formation of the potent proximate carcinogen (−)-BP-7,8-diol (*1*, *3*). Therefore, focus has been on the metabolic fate of these dihydrodiols. Two competing pathways exist for the further activation of BP-7,8-diol. The first pathway involves the secondary epoxidation of the *trans*-dihydrodiol to form the bay region diol epoxide (+)-*anti*-BPDE (*5*). (±)-*anti*-BPDE will form N^2-deoxyguanosine adducts with DNA and is a potent bacterial and mammalian mutagen and potent tumorigen (*3*). The second pathway involves dihydrodiol dehydrogenase, members of the aldo−keto reductase (AKR) superfamily, which oxidize BP-7,8-diol to the corresponding *o*-quinone, BP-7,8-dione (*6*, *7*). The $NADP^+$-dependent oxidation of BP-7,8-diol by AKRs initially results in a ketol which spontaneously rearranges to form a catechol. The catechol is unstable and undergoes autoxidation in air. The first one-electron oxidation results in the formation of an *o*-semiquinone anion radical and hydrogen peroxide. The second one-electron oxidation produces the fully oxidized *o*-quinone and superoxide anion (Scheme 1; *8*). The resulting *o*-quinones are highly reactive Michael acceptors which can react with cellular nucleophiles including GSH, RNA, and DNA (*9*−*11*). This raises the issue of whether PAH *o*-quinones are detoxification products or activated metabolites.

The PAH *o*-quinones produced are highly reactive nucleophiles and yield bimolecular rate constants for the addition of GSH of $2.0 \times 10^6\ M^{-1}\ min^{-1}$ (*9*). They are also redox active and either undergo a two-electron nonenzymatic reduction to re-form the catechol or a one-electron enzymatic reduction to re-form the *o*-semiquinone anion radical (*12*, *13*). These events establish futile redox cycles in which the generation of ROS can be amplified multiple times. As a result of these properties PAH *o*-quinones are both cyto- and genotoxic. They are potent cytotoxins yielding LC_{50} values of 20−30 μM in rat and human hepatoma cells (*13*). Mechanisms of cytotoxicity include changes in redox state, *o*-semiquinone macromolecule damage, and GSH depletion. Their electrophilic properties enable them to form both stable and depurinating DNA adducts, while the production of ROS increases the formation of 8-oxo-dGuo and DNA strand scission (*14*, *15*). The latter event leads to the production of base propenals and malondialdehyde, which is a potent mutagen. Importantly, the formation of 8-oxo-dGuo can give straightforward routes to G to T transversions (*16*), which are among the most common mutations observed in *K-ras* and *p53* in human lung cancer (*17*, *18*). Since ROS are the causative agents in radiation-induced carcinogenesis, this pathway of PAH metabolism mediated by AKRs may account for the complete carcinogenicity of PAH.

A number of human AKRs have been reported to oxidize the model *trans*-dihydrodiol substrate, benzenedihydrodiol, and were purified to homogeneity from human liver cytosol. The enzymes were initially referred to as DD1−DD4 (dihydrodiol dehydrogenase 1−4) even though their specificity for PAH *trans*-dihydrodiols was not established. Subsequently, DD1 or 20α(3α)-HSD (AKR1C1), DD2 or bile acid binding protein (AKR1C2), DDx or type 2 3α-HSD (AKR1C3), and DD4 or chlordecone reductase (AKR1C4) were expressed as recombinant proteins and shown to oxidize (±)-BP-7,8-diol to BP-7,8-dione (*19*, *20*). However, DD3, which also oxidized benzenedihydrodiol, was identified as aldehyde reductase (AKR1A1) (*21*). This posed the intriguing possibility that this general metabolic enzyme may be involved in PAH activation.

AKR1A1 is widely distributed among all mammalian species (*22*). It can catalyze the reduction of a variety of aromatic and medium-chain aliphatic aldehydes to their corresponding alcohols (*23*, *24*). The most notable properties of aldehyde reductases include NADP(H) specificity and high catalytic efficiency for aromatic aldehydes (*p*-carboxybenzaldehyde, *p*-nitrobenzaldehyde, pyridine-3-aldehyde, and pyridine-4-aldehyde), D-glucuronate, short-chain aldoses, and the cancer therapeutic agent daunorubicin.

This study demonstrates for the first time that the recombinant human aldehyde reductase catalyzes the $NADP^+$-dependent oxidation of a wide variety of *trans*-dihydrodiol

Scheme 2: Structures of the *trans*-Dihydrodiol Metabolites of Polycyclic Aromatic Hydrocarbons

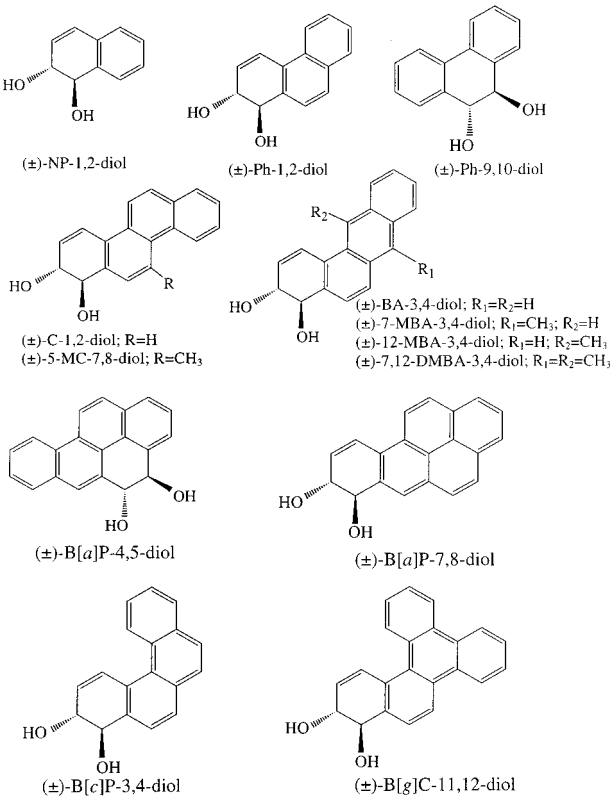

metabolites of PAH. The enzyme displays regioselectivity for the non-K-region *trans*-dihydrodiols. Aldehyde reductase was also highly stereoselective. It preferentially oxidized only 50% of the racemic PAH *trans*-dihydrodiols tested, including the metabolically relevant (−)-7*R*,8*R* enantiomer of BP-,7,8-diol. Aldehyde reductase catalyzed the oxidation of BP-7,8-diol to its corresponding *o*-quinone, BP-7,8-dione. Analysis of multiple tissue expression arrays showed coexpression of AKR1A1 with CYP1A1 and EH, suggesting that the formation of reactive and redox-active *o*-quinones may be widespread in human tissues.

MATERIALS AND METHODS

Chemicals and Reagents. $NADP^+$ and NADPH nucleotide cofactors were obtained from Boehringer Mannheim Biochemicals (Indianapolis, IN). DL-Glyceraldehyde and *p*-nitrobenzaldehyde were purchased from Sigma (St. Louis, MO). Recombinant AKR1C2 (2.5 μmol min^{-1} mg^{-1} using 1-acenaphthanol as substrate) and AKR1C4 (0.21 μmol min^{-1} mg^{-1} using androsterone as substrate) were purified to homogeneity (*19*).

trans-Dihydrodiol Synthesis. NP-1,2-diol was synthesized by reducing naphthalene-1,2-dione with sodium borohydride in ethanol (*25*). The K-region *trans*-diol, Ph-9,10-diol, was prepared by reducing phenanthrene-9,10-dione (Aldrich) with lithium aluminum hydride in ether (*26*). Other racemic *trans*-dihydrodiols were synthesized according to the methods cited in parentheses: BA-3,4-diol (*27*); 7-MBA-3,4-diol (*28*); 12-MBA-3,4-diol, 7,12-DMBA-3,4-diol (*29, 30*); C-1,2-diol (*31*); 5-MC-7,8-diol (*32*); BP-4,5-diol (*33*) (Scheme 2). (±)-BP-7,8-diol was purchased from the National Cancer Institute Chemical Carcinogen Reference Standard Repository at Chemsyn Science Laboratories (Lenexa, KS). All solvents were HPLC grade, and all other chemicals used were of the highest grade available.

Caution: All PAHs are potentially hazardous and should be handled in accordance with NIH Guidelines for the Laboratory Use of Chemical Carcinogens.

Oligonucleotide Synthesis and Isoform-Selective RT-PCR of AKR1A1 cDNA. The 5′-primer corresponded to 5′-dGGGGGCCATGGCGGCTTCCTG-3′ and contained an *Nco*I site (underlined) engineered at the ATG start codon, and the 3′ primer corresponded to 5′-dGTCTCAGTACGGGT-CATTAAAGGG-3′. The presence of the *Nco*I site facilitated in-frame subcloning of the PCR-amplified AKR1A1 coding region into the prokaryotic expression vector pET16b (Novagen).

A HepG2 first-strand cDNA library was prepared by isolating mRNA from a confluent 10 mm plate of HepG2 cells ($\sim 10^7$ cells) using Trizol reagent (Gibco BRL). Oligo-dT primers were added to 1 μg of a total RNA sample, and HepG2 mRNA was reverse transcribed using 200 units of Superscript II RNase H^- reverse transcriptase (Gibco BRL) at 55 °C for 2 h. Aliquots (1, 2, or 5 μL) of the first-strand cDNA library were mixed with 5′ and 3′ AKR1A1 specific primers (0.2 mM), dNTPs (0.4 mM), and 2 units of Vent DNA polymerase (NEB) in a final 1× reaction buffer volume of 50 μL. PCR was temperature-cycled using the following conditions: 94 °C for 1 min (denaturation), 50 °C for 1 min (annealing), and 72 °C for 1.5 min (extension) for 30 cycles. Following amplification, reaction mixtures were electrophoresed into a 1% agarose gel, and 1.0 kb fragments were isolated using the Qiaquick gel extraction kit (Qiagen).

Plasmid Constructs. PCR-amplified cDNA was ligated with T4 DNA ligase into the TA cloning vector pCRII (Invitrogen) using the Fast Link DNA ligation kit (Epicentre) to yield the pCRII-AKR1A1 construct. The identity of the positive insert was verified by dideoxysequencing in the Department of Genetics DNA sequencing facility at the University of Pennsylvania. The coding region in the SP6 orientation was excised from pCRII using *Nco*I and *Bam*HI and was directionally subcloned into the *Nco*I−*Bam*HI site of the prokaryotic expression vector pET16b. Utilization of the *Nco*I site in pET16b intentionally results in the excision of the histidine tag of the vector so that the expressed AKR1A1 contains only the desired amino acid sequence.

Prokaryotic Expression and Purification of AKR1A1. The pET16b-AKR1A1 construct was transformed into the *Escherichia coli* expression strain C41(DE3) (kindly provided by J. E. Walker of the Medical Research Council Laboratory of Molecular Biology, Cambridge, U.K.), grown to an OD of 0.6 at 600 nm, and then induced overnight with 1 mM IPTG. Bacterial sonicates were prepared and screened for the presence of AKR1A1 activity by measuring the reduction of *p*-nitrobenzaldehyde. SDS−PAGE confirmed the presence of an appropriately sized 37 kDa recombinant AKR1A1 protein in the bacterial sonicate.

Purification of AKR1A1 was achieved from a 4 L culture of C41(DE3) cells using the existing procedure for the purification of recombinant rat liver 3α-HSD/DD (*34*) following induction by 1 mM IPTG. Throughout the purification, peak fractions were collected, assayed with *p*-nitrobenzaldehyde, and visualized on SDS−PAGE with Coomassie Blue staining. Protein concentration was deter-

mined by the Bradford method. The final specific activity of AKR1A1 for *p*-nitrobenzaldehyde reduction was 6.0 μmol min^{-1} mg $^{-1}$ under standard assay conditions.

Kinetic Characterization of AKR1A1. K_m and V_{max} values for the reduction of DL-glyceraldehyde and *p*-nitrobenzaldehyde were obtained by varying the substrate concentration at a constant cofactor concentration (180 μM NADPH) in 1.0 mL systems containing 100 mM potassium phosphate buffer (pH 7.0) at 25 °C. DL-Glyceraldehyde was dissolved in water, and *p*-nitrobenzaldehyde was dissolved in acetonitrile. The final concentration of organic solvent in the assay was 4%. Initial velocities at each substrate concentration were measured on a Beckman DU640 spectrophotometer by measuring the change in absorbance of the pyridine nucleotide at 340 nm ($\epsilon = 6270$ M^{-1} cm $^{-1}$). Actual values of the kinetic constants were determined using ENZFITTER to fit untransformed data to a hyperbola which provides estimates of K_m and k_{cat} and their associated standard errors (*35*).

Spectrophotometric Assay of trans-Dihydrodiol Oxidation. The initial velocities of enzymatic oxidation of each *trans*-dihydrodiol substrate were determined spectrophotometrically using 2.3 mM NADP$^+$ as cofactor in 1.0 mL of 50 mM AMPSO buffer, pH 9.0 at 25 °C. The *trans*-dihydrodiol substrates were dissolved in DMSO, and the final concentration of organic solvent in the assay was 8%. Reactions were monitored by following the increase in absorbance of the reduced pyridine nucleotide at 340 nm on a Beckman DU 640 spectrophotometer. The specific activity for *p*-nitrobenzaldehyde was reduced 70% in the presence of 8% DMSO, and initial velocity data were corrected for this level of inhibition.

Stereochemical Course of trans-Dihydrodiol Oxidation. The stereochemical preference of the purified AKR1A1 for select racemic *trans*-dihydrodiol substrates was determined by CD spectroscopy. Reactions were run to completion, and the unreacted dihydrodiol was isolated for CD spectroscopy to determine the sign of the Cotton effect of the remaining isomer. Incubations were conducted in 10 mL systems containing 20−50 μM *trans*-dihydrodiol, 2.3 mM NADP$^+$, and 50 mM AMPSO buffer (pH 9.0) plus 8% DMSO. Following addition of the purified enzyme (~100 μg), the reactions were incubated at 25 °C overnight and then terminated by extraction of the dihydrodiols with ethyl acetate (3 × 10 mL aliquots). The organic solvent was dried with anhydrous sodium sulfate and then removed under reduced pressure. The resultant residues were chromatographed on 250 μm silica gel thin-layer chromatography plates using chloroform/ethyl acetate (1:1) as the running solvent. The unreacted diols were visualized under UV and extracted from the silica with ethanol to obtain sufficient material for CD ($A_{254nm} = 1.0$ OD unit). CD spectra were recorded on an Aviv model 60DS instrument at room temperature using a quartz cell with a 1 cm path length. CD spectra were plotted as millidegrees of ellipticity versus wavelength.

Characterization of the Product of Enzymatic Oxidation of BP-7,8-diol by Trapping with 2-Mercaptoethanol. To characterize the product of BP-7,8-diol oxidation catalyzed by AKR1A1, incubations were conducted in 50 mL systems containing 20 μM BP-7,8-diol, 2.3 mM NADP$^+$, 50 mM potassium phosphate buffer (pH 7.0), and 5 mM 2-mercaptoethanol plus 8% DMSO. Following addition of the purified enzyme (~1 mg), the reaction was incubated for 20 h at 37 °C and then terminated by extraction of the reaction mixture with ethyl acetate (2 × 50 mL aliquots). 2-Mercaptoethanol was added to the system to trap the presumptive reactive *o*-quinone as a more stable thioether conjugate. The organic extracts were combined and dried over sodium sulfate, and the organic solvent was removed under reduced pressure. The resulting solid was redissolved in methanol and was analyzed by LC/MS. The MS of the reaction product was compared to that obtained for the synthetically prepared BP-7,8-dione thioether conjugate (*7*). Mass spectrometric data were acquired on a Finnigan LCQ ion trap mass spectrometer (ThermoQuest, San Jose, CA) equipped with a Finnigan atmospheric pressure chemical ionization (APCI) source. The mass spectrometer was operated in the positive ion mode. On-line chromatography was performed using a Waters Alliance 2690 HPLC system (Waters Corp., Milford, MA). A YMC C_{18} ODS-AQ column was used at a flow rate of 0.9 mL/min. Solvent A was 5 mM ammonium acetate in water containing 0.01% trifluoroacetic acid, and solvent B was 5 mM ammonium acetate in methanol containing 0.01% trifluoroacetic acid with the gradient conditions as follows: 30% solvent B at 0 min, 30% solvent B at 5 min, 100% solvent B at 16 min, 100% solvent B at 24 min, and 30% solvent B at 26 min.

Multiple Tissue Expression Array. A dot blot containing poly(A)$^+$ RNA from multiple human tissues (CLONTECH) was hybridized to a randomly primed cDNA probe containing the entire open reading frame of AKR1A1. Random priming was achieved with radiolabeled [α-^{32}P]dATP, and a final specific activity greater than 10^9 cpm/μg of DNA was attained. Hybridization was performed at 65 °C for 6 h, and blots were washed with 2× standard saline citrate plus 1% SDS at 60 °C for 40 min. The blots were subjected to autoradiography at −70 °C. The blots were then stripped and reprobed. This was repeated for CYP1A1 [1 kb *Eco*RI fragment of the human CYP450 1A1 3′ untranslated region (phP1−450−3′, ATCC 63006)], epoxide hydrolase [1.8 kb *Sal*I−*Eco*RI fragment of the rat EH cDNA, pEH52 (kindly provided by C. B. Kasper, University of Wisconsin, Madison)], and a control housekeeping gene, ubiquitin. Data were analyzed and quantitated by phosphorimaging.

RESULTS

Prokaryotic Expression and Purification of Human Recombinant AKR1A1. The cDNA for human recombinant AKR1A1 was subcloned into the prokaryotic expression vector pET16b and overexpressed in the *E. coli* strain C41-(DE3). The protein was purified to homogeneity following induction by IPTG as described in Materials and Methods (Table 1). Homogeneous protein (30 mg) was obtained, the fold purification achieved was 4-fold, and the overall yield was 27%, reflecting the high level of expression achieved. Enzyme purity was established by SDS−PAGE followed by Coomassie staining (Figure 1).

Kinetic Characterization of Human Recombinant AKR1A1. Characterization of purified recombinant AKR1A1 was conducted using known standard substrates. The ability of AKR1A1 to reduce DL-glyceraldehyde and *p*-nitrobenzaldehyde with the concomitant oxidation of NADPH in 100 mM potassium phosphate buffer (pH 7.0) was measured. For DL-

Table 1: Purification Scheme for Recombinant Human Aldehyde Reductase (AKR1A1)

DD isoform	stage of purification	volume (mL)	protein (mg)	total activity (μmol/min)	specific activity (μmol min^{-1} mg^{-1})	fold purity	overall yield (% sonicate)
AKR1A1	sonicate	70	470	668	1.42	1	100
	DE52 cellulose	12.5	88.5	233	2.63	1.85	34.7
	Blue-Sepharose	7.1	30.5	183	6.0	4.23	27.4

[a] Specific activities were measured using 1 mM *p*-nitrobenzaldehyde as the substrate in reaction mixtures containing 100 mM potassium phosphate (pH 7.0) and 200 μM NADPH at 25 °C.

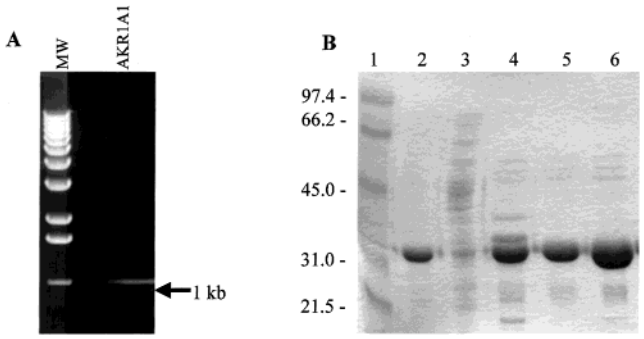

FIGURE 1: RT-PCR, cloning, expression, and purification of recombinant human AKR1A1. (A) RT-PCR of AKR1A1 cDNA. RT-PCR amplification from a HepG2 first-strand cDNA library was performed as described, and a 10 μL aliquot of the reaction mixture was electrophoresed on a 1% agarose gel stained with ethidium bromide to visualize the DNA band. (B) Expression and purification of recombinant human AKR1A1 from *E. coli* host cells. SDS−PAGE analysis: lane 1, MW marker; lane 2, 2 μg of AKR1A1 control; lane 3, 5 μg of bacterial cell sonicate; lane 4, 5 μg of the peak fraction from a DE52 cellulose column; lane 5, 5 μg of the peak fraction from a Blue-Sepharose affinity column (final step); lane 6, 10 μg of purified recombinant human AKR1A1.

Table 2: Substrate Specificity for Recombinant Human Aldehyde Reductase (AKR1A1)[a]

	DL-glyceraldehyde	*p*-nitrobenzaldehdyde
k_{cat} (min^{-1})	97 (78)	187 (306)
K_m (mM)	1.7 (1.7)	0.07 (0.16)
k_{cat}/K_m (min^{-1} M^{-1})	5.7×10^4 (4.6×10^4)	2.7×10^6 (1.9×10^6)

[a] Enzymatic reactions were performed in 100 mM potassium phosphate (pH 7.0) and 180 μM NADPH at 25 °C. Values (in parentheses) are taken from Barski et al. (*36*).

glyceraldehyde $k_{cat} = 97$ min^{-1}, $K_m = 1.7$ mM, and $k_{cat}/K_m = 5.7 \times 10^4$ M^{-1}min^{-1} was observed. For *p*-nitrobenzaldehyde $k_{cat} = 187$ min^{-1}, $K_m = 0.07$ mM, and $k_{cat}/K_m = 2.7 \times 10^6$ M^{-1}min^{-1} were determined. The catalytic efficiencies obtained were compared with values previously reported (*36*, *37*) for AKR1A1 (Table 2). This comparison revealed very good agreement between values for the recombinant enzyme and those previously reported for the native enzyme.

Initial Velocities of trans-Dihydrodiol Oxidation Catalyzed by AKR1A1. The limited solubility of the *trans*-dihydrodiols precluded direct determination of K_m and V_{max} values. To compare the ability of the purified AKR1A1 to oxidize *trans*-dihydrodiols, the initial velocity of the enzymatic oxidation of each potential substrate was measured at very low substrate concentrations, relative to K_m (less than 0.2 K_m). Since these reactions were conducted in the presence of saturating concentrations of NADP$^+$, the initial velocities observed under these conditions follow psuedo-first-order kinetics. In this instance, the Michaelis−Menten equation simplifies to $v/[s] = V_{max}/K_m$, providing a direct estimation of utilization ratio. Using this approach, utilization ratios were generated for the various *trans*-dihydrodiols with NADP$^+$ as coenzyme at pH 9.0. Values obtained were compared with the highest utilization ratios of other well-characterized human DDs (AKR1C1−AKR1C4) obtained under identical conditions (Table 3).

Table 3: Oxidation of Multiple Structurally Diverse PAH *trans*-Dihydrodiols by Human Aldehyde Reductase

PAH *trans*-dihydrodiols	V_{max}/K_m[a]
NP-1,2-diol	280 (4070 AKR1C1)
non-K-region dihydrodiols	
Ph-1,2-diol	484 (ND AKR1C1−4)
C-1,2-diol	420 (271 AKR1C4)
BA-3,4-diol	1840 (869 AKR1C4)
BP-7,8-diol	800 (235 AKR1C2)
methylated derivatives	
7-MBA-3,4-diol	2320 (1325 AKR1C2)
12-MBA-3,4-diol	ND (ND AKR1C1−4)
7,12-DMBA-3,4-diol	2625 (5000 AKR1C2)
5-MC-7,8-diol	3520 (952 AKR1C4)
K-region dihydrodiols	
Ph-9,10-diol	ND (ND AKR1C1−4)
BP-4,5-diol	ND (ND AKR1C1−4)
Fjord-region dihydrodiols	
B[*c*]P-3,4-diol	320 (222 AKR1C4)
B[*g*]C-11,12-diol	304 (4446 AKR1C4)

[a] Enzymatic reactions were in 50 mM AMPSO (pH 9) with 2.3 mM NADP$^+$. The concentrations of PAH diol substrates used were as follows: 20 μM (Ph-1,2-diol, BA-3,4-diol, 7-MBA-3,4-diol, 7,12-DMBA-3,4-diol, BP-4,5-diol, BP-7,8-diol); 50 μM (NP-1,2-diol, C-1,2-diol, 5-MC-7,8-diol, B[*c*]P-3,4-diol, B[*g*]C-11,12-diol). ND = not detectable. V_{max}/K_m = (nmol min^{-1} mg^{-1})/[S] × 1000. Values were corrected for inhibition of enzyme activity by the 8% DMSO cosolvent.

PAH *trans*-dihydrodiols of increasing ring number were oxidized by AKR1A1 (naphthalene to benzo[*a*]pyrene) (Scheme 2). PAH *trans*-dihydrodiols containing three or more rings (phenanthrene to benzo[*a*]pyrene) can reside in K or non-K regions. AKR1A1 oxidized only non-K-region *trans*-dihydrodiols (compare Ph-1,2-diol with Ph-9,10-diol and BP-7,8-diol with BP-4,5-diol). PAH *trans*-dihydrodiols with methylated non-bay regions were oxidized with even higher utilization ratios than their parent PAH by AKR1A1 (compare C-1,2-diol with 5MC-7,8-diol and BA-3,4-diol with 7MBA-3,4-diol). When utilization ratios for AKR1A1 were compared with AKR1C1−AKR1C4, in general AKR1A1 was the more efficient catalyst. Importantly, AKR1A1 gave the highest utilization ratio for BP-7,8-diol. Fjord-region dihydrodiols benzo[*c*]phenanthrene-3,4-diol and benzo[*g*]-chrysene-11,12-diol were also substrates for AKR1A1.

Determination of the End Point of Enzymatic Oxidation of Racemic trans-Dihydrodiols by AKR1A1. To determine whether AKR1A1 catalyzed the complete oxidation of racemic *trans*-dihydrodiols, HPLC assays were developed. The disappearance of diol substrate over time in the presence of enzyme was monitored. Initial velocities were calculated

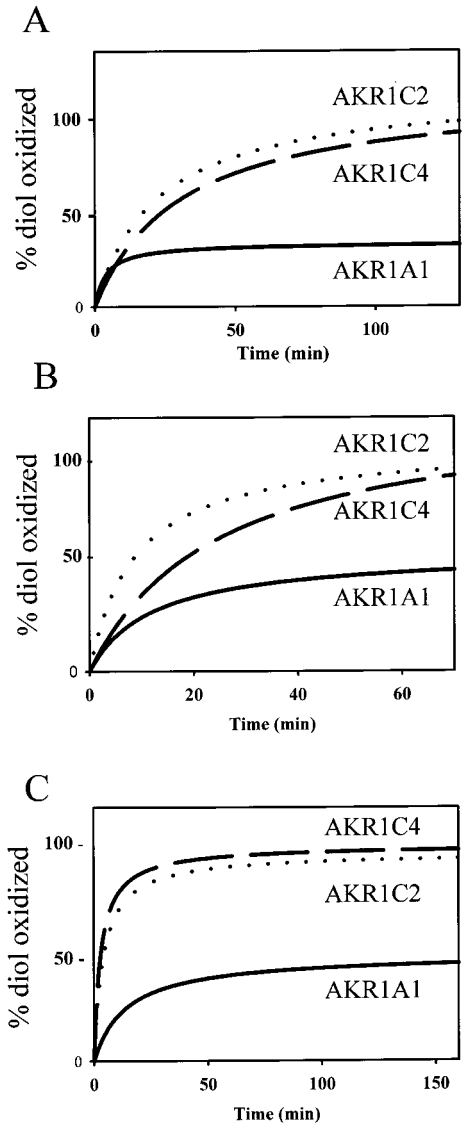

FIGURE 2: Determination of the end point of enzymatic oxidation of racemic *trans*-3,4-dihydrodiols of benz[*a*]anthracene by aldehyde reductase (AKR1A1) and two other human DD isoforms (AKR1C2 and AKR1C4). Progress curve for the oxidation of (A) BA-3,4-diol, (B) 7-MBA-3,4-diol, and (C) 7,12-DMBA-3,4-diol by human recombinant dihydrodiol dehydrogenase (AKR1A1, AKR1C2, and AKR1C4) isoforms. Racemic BA-3,4-diol, 7-MBA-3,4-diol, and 7,12-DMBA-3,4-diol (20 μM each) were incubated with AKR1A1 (4 μg), AKR1C2 (10 μg), or AKR1C4 (6 μg) in 50 mM AMPSO (pH 9.0) at 37 °C in the presence of 2.3 mM $NADP^+$. Initial velocities were determined by taking tangents to the progress curves.

by converting the peak area at each time point to nanomoles of dihydrodiol remaining and plotting these versus time. Reactions were carried out until no further change in peak area was observed; at this time the addition of a second aliquot of enzyme resulted in no further change in peak area, confirming that each reaction had reached completion. Progress curves for these reactions were computed and are shown in Figures 2A,B and 3A,B. These progress curves were compared with those obtained for AKR1C2 and AKR1C4 for the oxidation of BA-3,4-diol, 7-MBA-3,4-diol, and 7,12-DMBA-3,4-diol. In each instance, AKR1C2 and AKR1C4 oxidized 100% of the racemic *trans*-dihydrodiol substrate. By contrast, AKR1A1 oxidized only 50% of the racemic *trans*-dihydrodiols, suggesting stereochemical preference for a single stereoisomer.

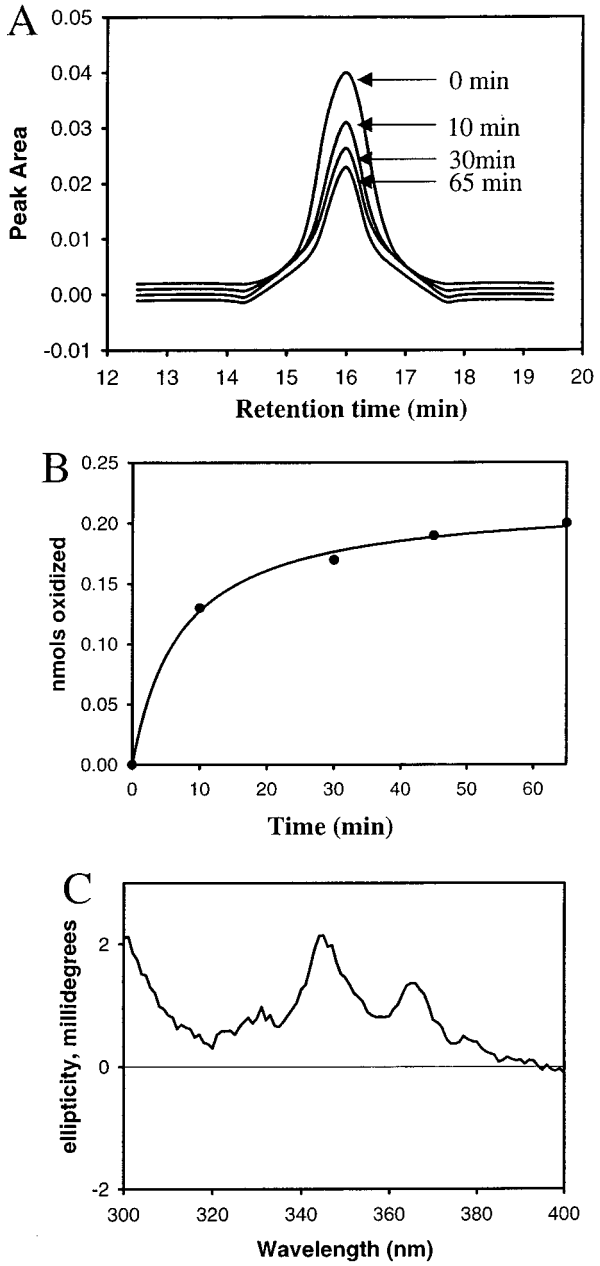

FIGURE 3: Oxidation of (±)-BP-7,8-diol by AKR1A1. (A) RP-HPLC assay of (±)-BP-7,8-diol oxidation catalyzed by AKR1A1. Racemic BP-7,8-diol (20 μM) was incubated with AKR1A1 (4.0 μg) in 50 mM AMPSO (pH 9.0) at 37 °C in the presence of 2.3 mM $NADP^+$. Chromatograms were obtained at different time points (0, 10, 30, 65 min, etc.). (B) Initial progress curve for the oxidation of (±)-BP-7,8-diol by AKR1A1. Initial velocities were calculated from the linear portion of the curve. (C) Identification of the BP-7,8-diol stereoisomer preferentially oxidized by AKR1A1. CD spectrum of unreacted dihydrodiol recovered from the AKR1A1-catalyzed reaction.

Identification of the Stereoisomer of BP-7,8-diol Preferentially Oxidized by AKR1A1. To identify the stereoisomer preferentially oxidized by AKR1A1, a large-scale reaction was conducted using (±)-BP-7,8-diol, and the enzymatic reaction was run to completion, i.e., until 50% of the racemate was consumed. The unreacted *trans*-dihydrodiol was extracted with ethyl acetate and was isolated by thin-layer chromatography. The recovered dihydrodiol was redissolved to give 1.0 AU/mL at the wavelength of maximum absorbance, and the CD spectra were recorded. The CD

spectra of the unreacted BP-7,8-diol gave a positive Cotton effect, indicating that the (−)-7*R*,8*R* isomer was preferentially oxidized (Figure 3C). Similar experiments were conducted for BA-3,4-diol, 7-MBA- 3,4-diol, and 7,12-DMBA-3,4-diol (data not shown). The (−)-3*R*,4*R* isomer of BA-3,4-diol, (+)-3*S*,4*S* isomer of 7MBA-diol, and (−)-3*R*,4*R* isomer of DMBA-3,4-diol were also found to be preferentially oxidized by AKR1A1.

Characterization of the Product of AKR1A1-Mediated Oxidation of BP-7,8-diol. To identify the product of BP-7,8-diol oxidation catalyzed by AKR1A1, a 50 mL reaction was conducted in the presence of 2-mercaptoethanol (see Materials and Methods). The anticipated product of the reaction, BP-7,8-dione, is a highly reactive Michael acceptor that can readily form conjugates with the buffer. Therefore, 2-mercaptoethanol was added as a strong nucleophile to trap the *o*-quinone as a thioether conjugate. The thiol attacks at C10 on BP-7,8-dione, forming a substituted ketol. The ketol undergoes keto−enol rearrangement to the catechol which autoxidizes to the substituted *o*-quinone. A synthetic standard was prepared by reacting BP-7,8-dione with 2-mercaptoethanol as previously described (*7*). LC/MS showed that the major enzymatic reaction product gave the same LC retention time and MS ions [$m/z = 359$ (MH^+) and $m/z = 331$ ($MH^+ - CO$)] as the synthetic standard identifying the reaction product as BP-7,8-dione. By contrast, LC/MS of BP-7,8-diol gave $m/z = 269$ ($MH^+ - H_2O$).

Coexpression of AKR1A1, CYP1A1, and Epoxide Hydrolase. To examine the expression of AKR1A1 in human tissues, a commercial Northern blot containing RNA from 16 different human tissues was probed with human AKR1A1 and then with human GAPDH cDNAs to normalize for equal loading (data not shown). AKR1A1 was present in every tissue with the highest expression being observed in the kidney, liver, small intestine, and pancreas. This result is consistent with the previously published data describing ubiquitous expression of human AKR1A1 (*38*).

Multiple tissue expression arrays were also probed to examine the coexpression of AKR1A1 with CYP1A1 and EH, the other two obligate enzymes required for the activation of parent PAH by this pathway. MTE array had 96 wells containing RNA from various human tissues and cell lines. The detection of AKR1A1, CYP1A1, EH, and ubiquitin was performed sequentially using the corresponding cDNA probes. This method allowed the distribution of a single enzyme to be measured across each tissue. However, the relative levels of each enzyme within a given tissue cannot be compared or quantitated. Data are shown from representative tissues (Figure 5).

Expression of AKR1A1 varied several-fold across human tissues. Highest levels were observed in kidney, liver, salivary gland, trachea, stomach, and fetal lung, which is consistent with the data obtained previously using Northern blot analysis. Thus AKR1A1 was expressed in every human tissue examined with highest levels seen in drug-metabolizing and PAH-exposed tissues. Although CYP1A1 is not an abundantly expressed CYP, it was expressed in the following rank order: liver > placenta > bladder > kidney > stomach > trachea. Its expression level varied approximately 10-fold across human tissues. The expression level of EH across human tissues was much more constant and varied approximately 3-fold. EH had the highest expression in salivary gland followed by trachea, testis, liver, prostate, and stomach. The blot was also probed with a housekeeping gene, ubiquitin (data not shown), to confirm uniform loading of poly(A)$^+$ RNAs.

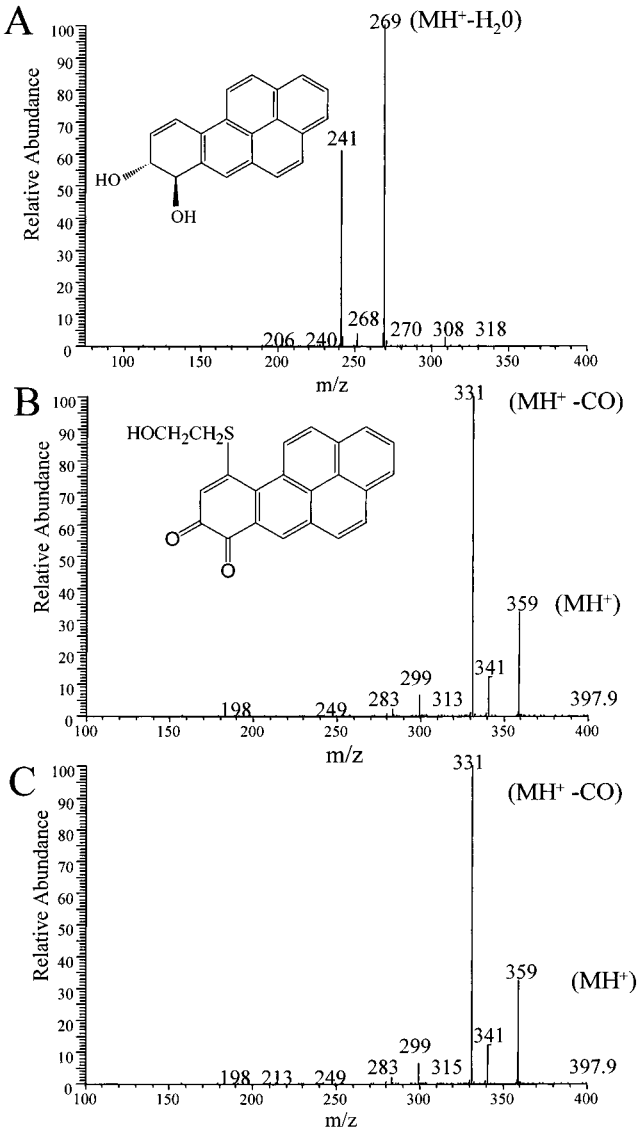

FIGURE 4: Characterization of the product of AKR1A1-catalyzed oxidation of BP-7,8-diol by LC/MS. LC/MS of (A) synthetic BP-7,8-diol, $m/z = 269$ ($MH^+ - H_2O$), (B) BP-7,8-dione thioether conjugate synthetically prepared from the reaction of BP-7,8-dione with 2-mercaptoethanol, $m/z = 359$ (MH^+) and $m/z = 331$ ($MH^+ - CO$), and (C) BP-7,8-dione thioether conjugate formed from the enzymatic oxidation of BP-7,8-diol by AKR1A1 in the presence of 2-mercaptoethanol, $m/z = 359$ (MH^+) and $m/z = 331$ ($MH^+ - CO$).

DISCUSSION

This report is the first demonstration of the substrate specificity of human aldehyde reductase (AKR1A1) for *trans*-dihydrodiol metabolites of PAH. Aldehyde reductase catalyzes the NADP$^+$-dependent oxidation of PAH *trans*-dihydrodiols of increasing ring number with different ring arrangements. Aldehyde reductase is one of the most abundantly expressed AKRs in human tissues. Physiologically, AKR1A1 catalyzes the reduction of mevaldate to mevalonic acid and glyceraldehyde to glycerol, which in turn is incorporated into triglyceride via the action of glycerol

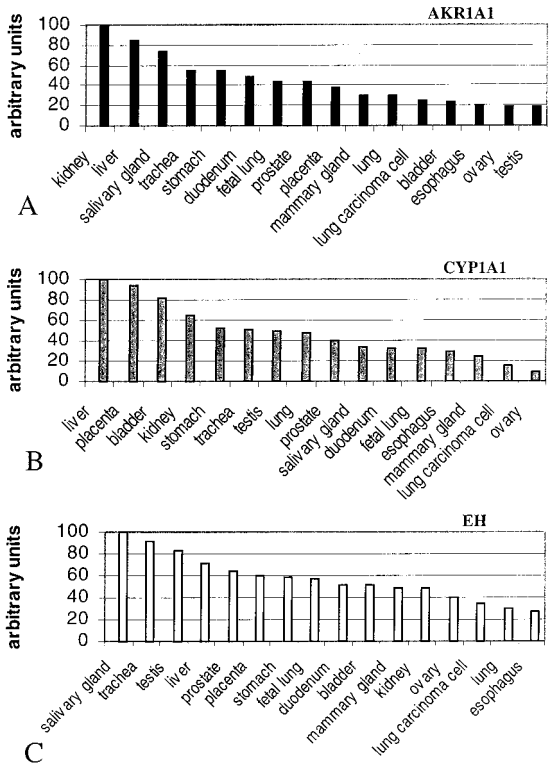

FIGURE 5: Coexpression of AKR1A1, CYP1A1, and epoxide hydrolase. Multiple tissue expression array data showing coexpression of the enzymes in PAH target tissues (A) probed with cDNA of human AKR1A1, (B) probed with the 3′-UTR of CYP1A1, and (C) probed with the cDNA of rat epoxide hydrolase. Following phosphorimaging analysis, the expression of each enzyme was plotted as a percent of that seen in the most abundant tissue.

kinase. These reactions demonstrate the involvement of AKR1A1 in the cholesterol and triglyceride biosynthetic pathways, respectively. Our data support a role of this general metabolic enzyme in PAH activation, which is further supported by data to indicate that it is coexpressed with CYP1A1 and EH.

If AKR1A1 plays a role in the further metabolic activation of PAH *trans*-dihydrodiols, it should show a preference for the oxidation of non-K-region (−)-*R,R*-*trans*-dihydrodiols. It was found that the K-region *trans*-dihydrodiols, BP-4,5-diol and Ph-9,10-diol, were not substrates while aldehyde reductase displayed regioselectivity for non-K-region *trans*-dihydrodiols. It catalyzed the oxidation of *trans*-dihydrodiols located on the terminal benzo ring as in the case of BP-7,8-diol. AKR1A1 therefore displays the appropriate regioselectivity to oxidize the potent proximate carcinogen non-K-region *trans*-dihydrodiols that arise metabolically.

The tumorigenic potential of many PAHs can be greatly enhanced by the presence of a methyl group on the parent hydrocarbon. In the chrysene series, its 5-methylated derivative compares favorably with the carcinogenicity of benzo[*a*]pyrene while the unmethylated hydrocarbon is not a carcinogen (*39*). Comparison of the utilization ratios of AKR1A1 for the oxidation of *trans*-dihydrodiols of the parent chrysene and its 5-methylated derivative shows rate enhancement of more than 8-fold as a result of methylation.

In the case of benz[*a*]anthracene, the parent compound is only a weak tumorigen while 7-methyl and 7,12-dimethyl derivatives have greatly enhanced carcinogenicity (*40*). AKR1A1 oxidized *trans*-dihydrodiols of the 7-methyl and 7,12-dimethyl derivatives with higher utilization ratios than *trans*-dihydrodiols of the parent hydrocarbon. It did not oxidize the *trans*-dihydrodiol of the bay region methylated 12-MBA-3,4-diol, showing preference for the non-bay region methylated diols in this series.

Importantly, AKR1A1 oxidized the potent proximate carcinogen (±)-BP-7,8-diol with a higher utilization ratio than any other AKR so far examined. It also showed stereospecificity for this diol and oxidized the metabolically formed (−)-7*R*,8*R* isomer exclusively. AKR1A1 was also stereospecific in its oxidation of BA *trans*-dihydrodiols. CD spectroscopy studies revealed that the (−)-3*R*,4*R* isomer of BA-3,4-diol, (+)-3*S*,4*S* isomer of 7-MBA-3,4-diol, and (−)-3*R*,4*R* isomer of 7,12-DMBA-3,4-diol were the isomers preferentially oxidized by AKR1A1. Thus AKR1A1 will oxidize the correct isomer of BA-3,4-diol formed in vivo. Both isomers of 7,12-DMBA-3,4-diol are formed upon activation of the parent hydrocarbon by human microsomes while AKR1A1 will preferentially oxidize the 3*R*,4*R* isomer. By contrast, although AKR1A1 will oxidize the 3*S*,4*S* isomer of 7-MBA-3,4-diol, the stereochemistry of the isomer produced by human microsomes in vitro is unknown. In summary, AKR1A1 will oxidize the relevant *trans*-dihydrodiol stereoisomers of BP, BA, and 7,12-DMBA.

A number of *trans*-dihydrodiols oxidized by AKR1A1 gave utilization ratios which do not correlate with their potency as proximate carcinogens in vivo. Compare BA-3,4-diol to BP-7,8-diol and BP-7,8-diol to B[*g*]C-11,12-diol. Several explanations may exist for these findings and may include other enzymes that may compete for these diols. This may be reflected by tissue expression profiles of CYP (CYP1A1-CYP1B1) and AKR isoforms (AKR1C1−AKR1C4).

Although AKR1C1−AKR1C4 (human dihydrodiol dehydrogenases of the 1C subfamily) and AKR1C9 (rat dihydrodiol dehydrogenase) have been shown to oxidize BP-7,8-diol to BP-7,8-dione, the reaction product formed by AKR1A1 was unknown. Using 2-mercaptoethanol as a trapping agent the product of BP-7,8-diol oxidation catalyzed by AKR1A1 was identified to be BP-7,8-dione by LC/MS.

Northern analysis of AKR1A1 showed high expression of AKR1A1 in kidney, liver, small intestine, and pancreas, which is consistent with the distribution previously published (*38*). MTE arrays were probed to determine whether AKR1A1 is coexpressed with CYP1A1 and EH, the other two enzymes required to make its *trans*-dihydrodiol substrates. To our knowledge MTE arrays have not been previously conducted for CYP1A1, EH, or AKR1A1 expression. Our results show that CYP1A1, EH, and AKR1A1 are all coexpressed. Examination of the expression profiles of the individual enzymes shows that AKR1A1 was detected in every tissue and cell line, with highest expression observed in kidney, drug-metabolizing tissues, e.g., liver, stomach, and duodenum, and PAH-exposed sites, e.g., salivary gland, trachea, lung, lung carcinoma cells, and esophagus. Its high expression in these sites suggests that this enzyme might be involved in xenobiotic metabolism and PAH activation. The high expression of AKR1A1 in kidney could be related to a role in the regulation of osmolarity as previously suggested (*38*).

CYP1A1 was expressed relatively highly in liver, placenta, bladder, kidney, stomach, and trachea (Figure 5B). Previous studies have shown basal expression of CYP1A1 in human

liver, lung, and pulmonary carcinomas (*41*). CYP1A1 is induced by planar aromatics, 3-methylcholanthrene and β-naphthoflavone, and various PAHs through transcriptional activation by up to 10-fold (*42*, *43*). However, no donor identities exist for the MTE to correlate expression levels with prior PAH exposure. Cigarette smoke will also induce CYP1A1 gene expression in normal human lung tissue (*44*), suggesting that PAH induce their own metabolism. Moreover, high CYP1A1 gene expression has been documented in many pulmonary carcinomas, and altered regulation of this gene was also observed in several lung tumors (*41*). Polymorphisms in CYP1A1 that increase its activity have also been seen in some lung carcinomas (*45*). Thus the level of CYP1A1 expression and its inducibility and possibly its allelic variations may support its role in PAH activation and its association with lung cancer.

EH, the other enzyme required for PAH *trans*-dihydrodiol formation, was also coexpressed with AKR1A1 and CYP1A1 in PAH target tissues such as liver, salivary gland, lung, and trachea. Previous studies demonstrated EH expression in a variety of human tissues including lung. Polymorphisms in exons 3 and 4 of EH gene have been reported in lung cancer where EH activity was increased (*46*).

Our findings implicate AKR1A1, CYP1A1, and EH in the metabolic activation of PAH. Understanding the mechanism of PAH activation in humans will ultimately lead to a thorough analysis of the expression levels and polymorphisms that exist in all relevant genes. Such an analysis will determine whether this variation reflects susceptibility to lung cancer. The interpretation of the functional consequences of such polymorphisms will be aided by the available crystal structures for AKR1A1 (*47*).

AKR1A1 like AKR1C1−AKR1C4 and AKR1C9 produces PAH *o*-quinones which fall into three classes with respect to their cyto- and genotoxic properties. 7,12-Dimethybenz[*a*]anthracene-3,4-dione (class I quinones) will produce large quantities of $O_2^{\bullet-}$ and SQ and decrease cell viability and cell survival by changing redox state; benz[*a*]-anthracene-3,4-dione (class II quinone) reduces cell survival only by the formation of SQ while BPQ (class III quinone) produces $O_2^{\bullet-}$ only and decreases cell viability via a mechanism that involves GSH depletion. These quinones can also mediate a spectrum of DNA-damaging events including the formation of stable and depurinating adducts and oxidative DNA lesions (*8*). The propensity of class I and class III *o*-quinones to produce ROS can also lead to the formation of oxidatively damaged bases, e.g., 8-oxo-dGuo (*15*). Collectively, these DNA-damaging events may contribute to PAH carcinogenesis (*8*). The ability of AKR1A1 to produce these cyto- and genotoxic end points in a cellular context can be addressed by treating AKR1A1 stable transfectants with *trans*-dihydrodiols that correspond to each of the three classes of *o*-quinones.

In summary, we provide evidence that a constitutively and widely expressed human AKR, namely, AKR1A1, can oxidize PAH *trans*-dihydrodiol metabolites to yield reactive and redox-active *o*-quinones. AKR1A1 oxidized several of the potent proximate carcinogen *trans*-dihydrodiols including BP-7,8-diol with higher utilization ratios than any other human AKR tested to date. The enzyme is regio- and stereoselective for PAH *trans*-dihydrodiols. It preferentially oxidized the metabolically relevant 7*R*,8*R* isomer of BP-7,8-diol to BP-7,8-dione, demonstrating its probable importance in vivo. AKR1A1 is coexpressed with CYP1A1 and EH in PAH target tissues. Together, these findings indicate that this ubiquitous enzyme might play a major role in PAH activation.

ACKNOWLEDGMENT

We thank Dr. Gopishetty R. Sridhar for the synthesis of the benzo[*a*]pyrene-7,8-dione thioether conjugate standard and Dr. Seon Hwa Lee for the mass spectrometric analysis.

REFERENCES

1. Conney, A. H. (1982) G. H. A. Clowes memorial lecture, *Cancer Res. 42*, 4875−4917.
2. Hoffmann, D., Djordjevic, V., and Hoffmann, I. (1997) *Prev. Med. 26*, 427−434.
3. Gelboin, H. V. (1980) *Physiol. Rev. 60*, 1107−1166.
4. Cavalieri, E. L., and Rogan, E. G. (1995) *Xenobiotica 25*, 677−688.
5. Yang, S. K., McCourt, D. W., Roller, P. P., and Gelboin, H. V. (1976) *Proc. Natl. Acad. Sci. U.S.A. 73*, 2594−2598.
6. Smithgall, T. E., Harvey, R. G., and Penning, T. M. (1986) *J. Biol. Chem. 261*, 6184−6191.
7. Smithgall, T. E., Harvey, R. G., and Penning, T. M. (1988) *J. Biol. Chem. 263*, 1814−1820.
8. Penning, T. M., Burczynski, M. E., Hung, C.-F., McCoull, K. D., Palackal, N. T., and Tsuruda, L. S. (1999) *Chem. Res. Toxicol. 12*, 1−18.
9. Murty, V. S., and Penning, T. M. (1992) *Chem.-Biol. Interact. 84*, 169−188.
10. Shou, M., Harvey, R. G., and Penning, T. M. (1993) *Carcinogenesis 14*, 475−482.
11. McCoull, K. D., Rindgen, D., Blair, I. A., and Penning, T. M. (1999) *Chem. Res. Toxicol. 12*, 237−246.
12. Flowers-Geary, L., Harvey, R. G., and Penning, T. M. (1992) *Biochem. (Life Sci.) 11*, 49−58.
13. Flowers-Geary, L., Bleczinski, W., Harvey, R. G., and Penning, T. M. (1996) *Chem.-Biol. Interact. 99*, 55−72.
14. Flowers, L., Ohnishi, S. T., and Penning, T. M. (1997) *Biochemistry. 36*, 8640−8648.
15. Glaze, E. R., Flowers, L., and Penning, T. M. (2001) *Proc. Am. Assoc. Cancer Res. 42*, 2540.
16. Zhang, Y., Yuan, F., Wu, X., Rechkoblit, O., Taylor, J.-S., Geacintov, N. E., and Wang, Z. (2000) *Nucleic Acids Res. 28*, 4717−4724.
17. Rodenhuis, S. (1992) *Semin. Cancer Biol. 3*, 241−247.
18. http://perso.curie.fr/Thierry.Soussi/p53_mutation_in_%20lung.html.
19. Burczynski, M. E., Harvey, R. G., and Penning, T. M. (1998) *Biochemistry 37*, 6781−6790.
20. Burczynski, M. E., Palackal, N. T., Harvey, R. G., and Penning, T. M. (1999) *Polycyclic Aromat. Compd. 16*, 205−214.
21. Hara, A., Taniguchi, H., Nakayama, T., and Sawada, H. (1990) *J. Biochem. 108*, 250−254.
22. Davidson, W. S., Walton, D. J., and Flynn, T. G. (1978) *Comp. Biochem. Physiol. 60B*, 309−315.
23. Wermuth, B., Munch, J. D., and Von Wartburg, J. P. (1977) *J. Biol. Chem. 252*, 3821−3828.
24. Flynn, G. T. (1982) *Biochem. Pharmacol. 31*, 2705−2712.
25. Platt, K. L., and Oesch, F. (1983) *J. Org. Chem. 48*, 265−268.
26. Cortez, C., and Harvey, R. G. (1978) *Org. Synth. 58*, 12−16.
27. Harvey, R. G., and Sukumaran, K. B. (1977) *Tetrahedron Lett.* 2387−2390.
28. Lee, H. H., and Harvey, R. G. (1979) *J. Org. Chem. 44*, 4948−4953.
29. Sukumaran, K. B., and Harvey, R. G. (1980) *J. Org. Chem. 45*, 4407−4413.
30. Lee, H. H., and Harvey, R. G. (1986) *J. Org. Chem. 51*, 3502−3507.
31. Fu, P. P., and Harvey, R. G. (1979) *J. Org. Chem. 44*, 3778−3784.

32. Pataki, J., Lee, H. H., and Harvey, R. G. (1983) *Carcinogenesis 4*, 399−402.
33. Harvey, R. G., Gosh, S. H., and Cortez, C. (1975) *J. Am. Chem. Soc. 97*, 3468−3479.
34. Jez, J. M., Schlegel, B. P., and Penning, T. M. (1996) *J. Biol. Chem. 271*, 30190−30196.
35. Leatherbarrow, R. J. (1987) *ENZFITTER: A Non-Linear Regression Data Analysis Program for the IBM PC (and true compatibles)*, Biosoft, Cambridge, U.K.
36. Barski, O. A., Gabbay, K. H., and Bohren, K. M. (1997) *Adv. Exp. Med. Biol. 414*, 443−451.
37. Barski, O. A., Gabbay, K. H., Grimshaw, C.E., and Bohren, K. M. (1995) *Biochemistry 34*, 11264−11275.
38. O'Connor, T., Ireland, L. S., Harrison, D. J., and Hayes, J. D. (1999) *Biochem. J. 343*, 487−504.
39. Hecht, S. S., Radok, L., Amin, S., Huie, K., Melikian, A. A., Hoffmann, D., Pataki, J., and Harvey, R. G. (1985) *Cancer Res. 45*, 1449−1452.
40. Wislocki, P. G., Gadek, K. M., Chou, M. W., Yang, S. K., and Lu, A. Y., (1980) *Cancer Res. 40, 3661−36644.*
41. McLemore, T. L., Adelberg, S., Liu, M. C., McMohan, N. A., Yu, S. J., Hubbard, W. C., Czerwinski, M., Wood, T. G., Storeng, R., Lubet, R. A., Eggleston, J. C., Boyd, M. R., and Hines, R. N. (1990) *J. Natl. Cancer Inst. 82*, 1333−1339.
42. Omiecinski, C. J., Redlich, C. A., and Costa, P. (1990) *Cancer Res. 50*, 4315−4321.
43. Denison, M. S., and Whitlock J. P. (1995) *J. Biol. Chem. 270*, 18175−18178.
44. Willey, J. C., Coy, E. L., Frampton, M. W., Torres, A., Apostolakos, M. J., Hoehn, G., Schuermann, W. H., Thilly, W. G., Olson, D. E., Hammersley, J. R., Crespi, C. L., and Utell, M. J. (1997) *Am. J. Respir. Cell Mol. Biol. 17*, 114−124.
45. Lin, P., Wang, S. L., Wang, H. J., Chen, K. W., Lee, H. S., Tsai, K. J., Chen, Y. C., and Lee, H. (2000) *Br. J. Cancer 82*, 852−857.
46. Benhamou, S., Reinikainen, M., Bouchardy, P. D., and Hirvonen, A. (1998) *Cancer Res. 58*, 5291−5293.
47. el-Kabbani, O., Judge, K., Ginell, S.L., Myles, D.A., DeLucas, L. J., and Flynn, T. G. (1995) *Nat. Struct. Biol. 2*, 687−692.

BI010872T